



## Negative Gilbert damping

Yunshan Cao and Peng Yan <sup>\*</sup>

*School of Electronic Science and Engineering and State Key Laboratory of Electronic Thin Films and Integrated Devices, University of Electronic Science and Technology of China, Chengdu 610054, China*

 (Received 3 August 2021; revised 20 January 2022; accepted 7 February 2022; published 14 February 2022)

Modern ferromagnetism theory is based on the Landau-Lifshitz-Gilbert equation that governs the dynamics of magnetic moment in a ferromagnet. As a deep-rooted notion, the Gilbert damping parameter must be positive because it describes the (energy and angular momentum) dissipation. In this paper, we report a negative Gilbert damping via the magneto-optical interaction of three orthogonal circularly-polarized laser beams with a submicron magnet placed in an optical cavity. We show that the off-resonant coupling between the driving laser and cavity photon in the far-blue detuning can induce a magnetic torque exactly of the Gilbert type with negative damping coefficient. A hyperbolic-tangent function ansatz is found to well describe the time-resolved spin switching as the intrinsic dissipation is overcome. Feasible experiments and materials are discussed to test our theory.

DOI: [10.1103/PhysRevB.105.064418](https://doi.org/10.1103/PhysRevB.105.064418)

### I. INTRODUCTION

The Landau-Lifshitz-Gilbert (LLG) equation is the cornerstone of the phenomenological theory of magnetism [1]. It successfully describes multiscale magnetization dynamics, ranging from biocompasses that sense the geomagnetic field [2], to magnetic hard disks that store binary information [3], and to solitons that are robust against external frustrations [4]. The standard LLG equation takes the following form:

$$\frac{\partial \mathbf{M}}{\partial t} = -\gamma \mathbf{M} \times \mathbf{H}_{\text{eff}} + \frac{\alpha}{|\mathbf{M}|} \mathbf{M} \times \frac{\partial \mathbf{M}}{\partial t}, \quad (1)$$

where  $\mathbf{M} = -\gamma \mathbf{S}$  is the local magnetization with spin momentum  $\mathbf{S}$ ,  $\gamma > 0$  is the gyromagnetic ratio, and  $\mathbf{H}_{\text{eff}}$  is the effective field around which the local magnetization precesses.  $\alpha$  is the Gilbert damping parameter describing the dissipation of energy and angular momentum, and it thus must be positive, as a well-established notion. A smaller Gilbert damping corresponds to a higher quality of magnetic solids [5]. Yttrium iron garnet (YIG) is the known material with the lowest magnetic damping ( $\alpha \sim 10^{-5}$ ) [6,7], but the quality factor ( $Q$  factor) is still far less than its optical and/or superconducting counterparts [8,9]. Pursuing materials with even smaller Gilbert damping is of vital importance to both fundamental magnetism and applied spintronics. For example, a very high magnon  $Q$  factor would enable the magnonic frequency comb [10] to eventually compete with the optical comb. However, there exist several intrinsic mechanisms, such as the relativistic spin-orbit coupling [11], spin-lattice interaction [12,13], and two-magnon scattering at surfaces [14], that hinder the success to further reduce the Gilbert damping. How to realize a Gilbert damping arbitrarily close to zero or even across the border (negative damping) is an interesting and challenging problem.

The past decade has witnessed the flourish of cavity spintronics that focuses on the resonant coupling between microwave cavity photons and magnons (quanta of spin waves) [15–21]. Thorough reviews on cavity magnonics and quantum magnonics can be found in Ref. [22] and Ref. [23], respectively. One recent trend beyond microwave is the parametric coupling of optical lasers with magnons, that generates interesting new opportunities, such as the nonreciprocal Brillouin light scattering [24], the microwave-to-optical converting [25,26], the optical cooling of magnons [27], etc. In these studies, considerable interests have been drawn to the scalar properties of magnons, e.g., magnon population, temperature, and chemical potential, which is successful to describe the small-angle spin precession enabling the Holstein-Primakoff transformation to quantize the spin dynamics in terms of magnons [28]. In contrast, their vectorial behavior, i.e., the full time-evolution of the magnetic moment in optical cavities driven by lasers, remains largely unexplored, with only few exceptions [29]. It has been shown that a ferromagnetic-to-antiferromagnetic phase transition may emerge in the vicinity of the magnonic exceptional point [30,31]. In such case, the magnetic moment would significantly deviate from its equilibrium direction, and a vectorial field description becomes more relevant than a scalar one.

In this paper, we propose an optomagnonic approach to realize the negative Gilbert damping. We consider the off-resonant interaction between three orthogonal circularly-polarized laser beams and a submicron magnet placed in an optical cavity [see Fig. 1(a)]. By solving the coupled equations of motion and integrating out the photon's degree of freedom, we derive the analytical formula of the optical torque acting on the macrospin. In the far-blue detuning, we find that the optical torque exactly takes the Gilbert form  $-\frac{\alpha_{\text{opt}}}{S} \dot{\mathbf{S}} \times \mathbf{S}$  with  $\alpha_{\text{opt}} > 0$  (see below). The total Gilbert damping becomes negative when the intrinsic dissipation is overcome. A hyperbolic-tangent function ansatz is found to well describe the time-resolved spin switching.

<sup>\*</sup>Corresponding author: yan@uestc.edu.cn

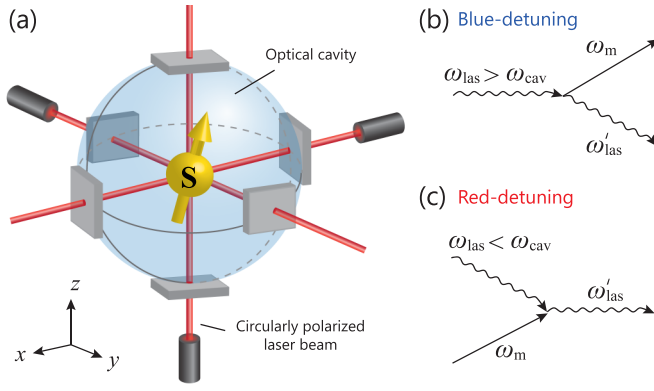


FIG. 1. (a) Schematic illustration of a macrosin  $\mathbf{S}$  interacting with three orthogonally propagating circularly-polarized lasers (red beams) in an optical cavity. Off-resonant coupling between the driving laser ( $\omega_{\text{las}}$ ) and the cavity photon ( $\omega_{\text{cav}}$ ) mediated by magnons ( $\omega_m \ll \omega_{\text{cav}}$ ) in the blue (b) and red (c) detuning regimes.

The paper is organized as follows. We present the general model in Sec. II. Main results are given in Sec. III, in which we derive the negative Gilbert damping torque and rationalize materials and experiments to test our theory. In Sec. IV, we discuss the indications and prospects of our proposal. The conclusion is drawn in Sec. V.

## II. MODEL

The proposed setup is schematically plotted in Fig. 1(a). Three circularly-polarized laser beams propagating respectively along  $x, y, z$  directions drive the parametric coupling with a macrosin  $\mathbf{S} = (\hat{S}_x, \hat{S}_y, \hat{S}_z)$  inside the optical cavity. The external magnetic field is applied along  $z$  axis. The total Hamiltonian in the rotating frame of reference at the pump laser frequency is expressed as (see Appendix A)

$$\mathcal{H} = -\hbar\omega_m\hat{S}_z - \hbar \sum_{j=x,y,z} (\Delta_j - g_j\hat{S}_j)\hat{c}_j^\dagger\hat{c}_j + \mathcal{H}_{\text{dr}}, \quad (2)$$

where the first term is the Zeeman energy, the second term is the magneto-optical interaction,  $\Delta_j = \omega_{\text{las},j} - \omega_{\text{cav}}$  is the frequency detuning between the cavity photon  $\omega_{\text{cav}}$  and the driving laser  $\omega_{\text{las},j}$ ,  $j = x, y, z$  denotes the three orthogonally-propagating laser beams, and  $\hat{c}_j^\dagger(\hat{c}_j)$  is the creation (annihilation) operator of the optical cavity photons. The coupling strength  $g_j = \frac{c\theta_F}{S\sqrt{\epsilon_r}}$  between the spin and optical photon originates from the Faraday-induced modification of the electromagnetic energy in ferromagnets [32], with  $S$  the total spin number,  $c$  being the speed of light in vacuum,  $\theta_F = \frac{fM_s\omega_{\text{las}}}{2c\sqrt{\epsilon_r}}$  being the Faraday rotation per unit length, and  $M_s$  being the saturated magnetization. In the following calculations, we assume a (driving) frequency-independent coupling by replacing  $\omega_{\text{las},j}$  with  $\omega_{\text{cav}}$  in  $\theta_F$ , which is justified since  $|\omega_{\text{las},j} - \omega_{\text{cav}}|/\omega_{\text{cav}} \ll 1$ . The last driving term describes the interaction between the driving laser and the cavity photon  $\mathcal{H}_{\text{dr}} = i\hbar \sum_j (A_j\hat{c}_j^\dagger - \text{H.c.})$ , where  $A_j = (2\kappa_j P_j/\hbar\omega_{\text{las},j})^{1/2}$  is the field amplitude, with  $\kappa_j$  the laser external loss rate and  $P_j$  being the driving power. The Heisenberg-Langevin

equations of motion for coupled photons and spins are expressed as ( $\partial \equiv (\partial)$ ),

$$\dot{c}_j = (i\Delta_j - \kappa_j)c_j - ig_j S_j c_j + A_j, \quad (3a)$$

$$\dot{S}_x = \omega_m S_y + g_y n_y S_z - g_z n_z S_y, \quad (3b)$$

$$\dot{S}_y = -\omega_m S_x - g_x n_x S_z + g_z n_z S_x, \quad (3c)$$

$$\dot{S}_z = -g_y n_y S_x + g_x n_x S_y, \quad (3d)$$

where  $n_j = \langle \hat{c}_j^\dagger \hat{c}_j \rangle$  is the average photon number in the cavity. Because the spin dynamics usually is much slower than optical photons, one can expand the cavity photon operator as  $c_j(t) \approx c_{j0}(t) + c_{j1}(t) + \dots$ , in orders of  $\dot{S}_j$ . Equation (3a) then can be recast in series (see Appendix B)

$$0 = (i\Delta_j - \kappa_j)c_{j0} - ig_j S_j c_{j0} + A_j, \quad (4a)$$

$$\dot{c}_{j0} = (i\Delta_j - \kappa_j)c_{j1} - ig_j S_j c_{j1}, \quad (4b)$$

by keeping up to the first-order terms. We can therefore derive the formula of photon number in the cavity  $n_j(t) \approx |c_{j0}|^2 + 2\text{Re}[c_{j0}^* c_{j1}]$ . Substituting it into Eqs. (3b)–(3d) and considering the intrinsic Gilbert damping [33], we obtain

$$\dot{\mathbf{S}} = -\gamma \mathbf{S} \times \mathbf{B}_{\text{eff}} + \frac{\alpha}{S} (\dot{\mathbf{S}} \times \mathbf{S}) - \boldsymbol{\beta}_{\text{opt}} \times \mathbf{S}, \quad (5)$$

where the effective magnetic field  $\mathbf{B}_{\text{eff}} = -B_0 \mathbf{e}_z + \mathbf{B}_{\text{opt}}$  includes both the external magnetic field  $-B_0 \mathbf{e}_z$  and the optically induced one

$$\mathbf{B}_{\text{opt}} = \sum_j \frac{\gamma^{-1} g_j A_j^2}{(\Delta_j - g_j S_j)^2 + \kappa_j^2} \mathbf{e}_j, \quad (6)$$

which is the zeroth-order of  $\dot{S}_j$ . The second term in the right-hand side of (5) is the intrinsic Gilbert damping torque with  $\alpha > 0$  [34]. The last term in (5) represents the optical torque with the anisotropic effective field

$$\boldsymbol{\beta}_{\text{opt}} = \sum_j \frac{4\kappa_j A_j^2 g_j^2 (\Delta_j - g_j S_j)}{[(\Delta_j - g_j S_j)^2 + \kappa_j^2]^3} \dot{S}_j \mathbf{e}_j, \quad (7)$$

which is linear with the first-order time-derivative of  $S_j$ . Below, we show that the anisotropic nature of (7) can be smeared out under proper conditions.

## III. RESULTS

### A. Negative Gilbert damping

To obtain the optical torque of exactly the Gilbert form, we make two assumptions: (i) the three laser beams are identical, i.e.,  $A_j = A$ ,  $g_j = g$ ,  $\kappa_j = \kappa$ , and  $\Delta_j = \Delta$ ; (ii) the optomagnonic coupling works in the far-detuning regime, i.e.,  $|\eta| \gg 1$  with  $\eta = \Delta/(gS)$ , which allows us to drop the  $g_j S_j$  terms in Eq. (7). The optically induced effective fields then take the simple form

$$\mathbf{B}_{\text{opt}} = \frac{\gamma^{-1} g A^2}{\Delta^2 + \kappa^2} \sum_j \mathbf{e}_j, \quad (8)$$

and

$$\boldsymbol{\beta}_{\text{opt}} = \frac{\alpha_{\text{opt}}}{S} \dot{\mathbf{S}}, \quad \text{with } \alpha_{\text{opt}} = \frac{4\kappa A^2 g^2 S \Delta}{(\Delta^2 + \kappa^2)^3} \quad (9)$$

TABLE I. Parameters for optical cavity and YIG.

cavity mode	cavity loss	Zeeman energy	MO coupling	Gilbert damping	Spin density	Faraday rotation
$\omega_{\text{cav}}/2\pi$	$\kappa/2\pi$	$\omega_m/2\pi$	$gS/2\pi$	$\alpha$	$\rho_s$	$\theta_F$
100 THz	1 GHz	10 GHz	1 GHz	$10^{-4}$	$10^{28}\text{m}^{-3}$	$188^\circ/\text{cm}$

being the laser-induced magnetic gain or loss that depends the sign of the detuning  $\Delta$ . Based on the above results, we finally obtain the optically modulated spin dynamics

$$\dot{\mathbf{S}} = -\gamma \mathbf{S} \times \mathbf{B}_{\text{eff}} + \frac{\alpha_{\text{eff}}}{S} (\dot{\mathbf{S}} \times \mathbf{S}), \quad (10)$$

with  $\alpha_{\text{eff}} = -\alpha_{\text{opt}} + \alpha$ . One can observe that a negative effective Gilbert constant ( $\alpha_{\text{eff}} < 0$ ) emerges in the far-blue detuning regime, i.e.,  $1 < \eta < \eta_c$ . In case of the red detuning ( $\eta < 0$ ), we have  $\alpha_{\text{opt}} < 0$ , which indicates the enhancement of the magnetic attenuation. In the deep-blue detuning regime ( $\eta > \eta_c$ ), driving lasers can still generate the magnetic gain ( $\alpha_{\text{opt}} > 0$ ) but cannot compensate the intrinsic dissipation, i.e.,  $0 < \alpha_{\text{opt}} < \alpha$ . Here  $\eta_c$  is the critical detuning parameter at which the effective Gilbert damping vanishes. The physics can be understood from the diagram plotted in Figs. 1(b) and 1(c): In the blue detuning regime ( $\omega_{\text{las}} > \omega_{\text{cav}}$ ), microwave magnons are emitted in the off-resonant interaction between the driving laser and the cavity photon, representing a magnetic gain. On the contrary, they are absorbed in the red detuning ( $\omega_{\text{las}} < \omega_{\text{cav}}$ ), manifesting a magnon cooling. Below we discuss practical materials and parameters to realize this proposal.

### B. Materials and experiments

For a ferromagnetic insulator like yttrium ion garnet (YIG), the intrinsic Gilbert constant  $\alpha$  typically ranges  $10^{-3} \sim 10^{-5}$  [6,7]. We take  $\alpha = 10^{-4}$  in the following calculations and estimations. The magneto-optical coupling strength is determined by the Faraday rotation coefficient  $\theta_F$  of the materials  $gS \simeq c\theta_F/\sqrt{\epsilon_r}$  (for YIG, we choose  $\epsilon_r = 15$  [35] and  $\theta_F = 188^\circ/\text{cm}$  [36]). Unlike the resonant case that the individual coupling keeps a constant and the total coupling is proportional to the square root of spin number [19], the magneto-optical coupling strength  $g$  here is inversely proportional to the total spin number  $S$  [28], because their product  $gS$  is fixed by the Faraday rotation coefficient.

We thus have  $gS/2\pi \approx 1$  GHz. The optical cavity is set at the resonant frequency  $\omega_{\text{cav}}/2\pi = 100$  THz with the loss rate  $\kappa/2\pi = 1$  GHz. For a YIG sphere of radius  $r = 10$  nm and spin density  $\rho_s \approx 10^{28} \text{m}^{-3}$ , we estimate the total spin number  $S = \rho_s r^3 \approx 10^4$  and the coupling strength  $g/2\pi \approx 0.1$  MHz. Materials parameters are summarized in Table I. Because  $g \ll \kappa$ , all interesting physics occurs in the weak-coupling regime. Considering the driving laser with a fixed power  $P = 1 \mu\text{W}$ , the effective Gilbert-type magnetic gain is  $\alpha_{\text{eff}} = -\alpha$  at  $\eta_{\text{PT}} \simeq 6.16$ , and the critical gain-loss point  $\alpha_{\text{eff}} = 0$  occurs at  $\eta_c \simeq 7.11$ , indeed satisfying the large-detuning condition  $|\eta| \gg 1$  in deriving (9). Figure 2(a) shows the monotonically decreasing dependence of the optically induced magnetic gain  $\alpha_{\text{opt}}$  on the detuning parameter  $\eta$ . The  $\eta$  dependence of the optical field is plotted in Fig. 2(b), showing that it monotonically

decreases with the increase of the detuning. Enhancing the laser power will push the two critical points  $\eta_c$  and  $\eta_{\text{PT}}$  into the deep detuning region, as demonstrated in Fig. 2(c). For a magnetic sphere of larger volume  $1 \mu\text{m}^3 \sim 1 \text{mm}^3$  that contains a total spin number  $S = 10^{10} \sim 10^{19}$  with the reduced magneto-optical coupling strength  $g/2\pi = 10^{-1} \sim 10^{-10}$  Hz, the required laser power then should be  $6 \sim 15$  orders of magnitude higher than that for nm-scale spheres, as shown in Fig. 2(d).

### C. Time-resolved spin flipping

To justify the approximation adopted in deriving the negative Gilbert damping torque, we directly simulate the time evolution of the unit spin components ( $s_j \equiv S_j/S$ ) based on both Eq. (5) and Eq. (10). Numerical results are, respectively, plotted in Figs. 3(a) and 3(b) for the same detuning parameter  $\eta = 1.8$  (corresponding to an effective damping  $\alpha_{\text{eff}} = -0.0453$ ) and  $\omega_m/2\pi = 10$  GHz. Both figures show that the very presence of the negative Gilbert damping can flip the spin in a precessional manner, with similar switching curves. The fast Fourier transformation (FFT) analysis of the temporal oscillation of  $s_x$  also confirms this point (see the insets). Although the analytical form of  $s_z(t)$  by solving (5) generally is unknown [37,38], we find an ansatz that can well describe the time-resolved spin switching

$$s_z(\tau) \simeq \tanh\left(-\frac{\tau - \tau_0}{\tau_p}\right), \quad (11)$$

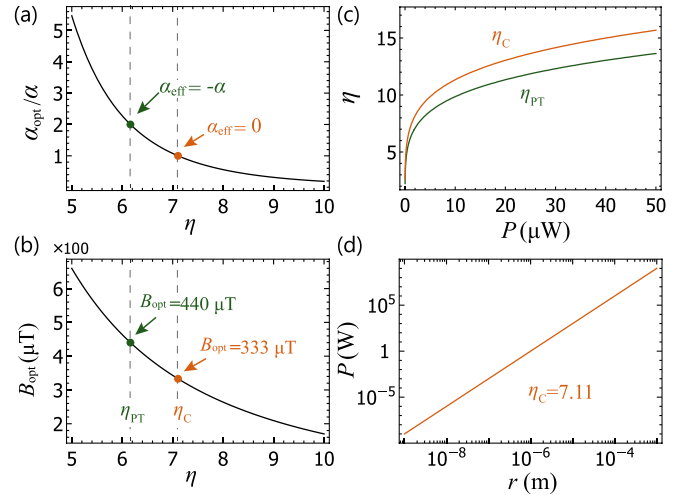


FIG. 2. Optically induced magnetic gain (a) and magnetic field (b) vs the optical detuning parameter  $\eta$ . (c)  $\eta_{\text{PT}}$  (orange) and  $\eta_c$  (green) as a function of the driving laser power. (d) Radius dependence of the laser power at the compensation point  $\eta_c = 7.11$ .

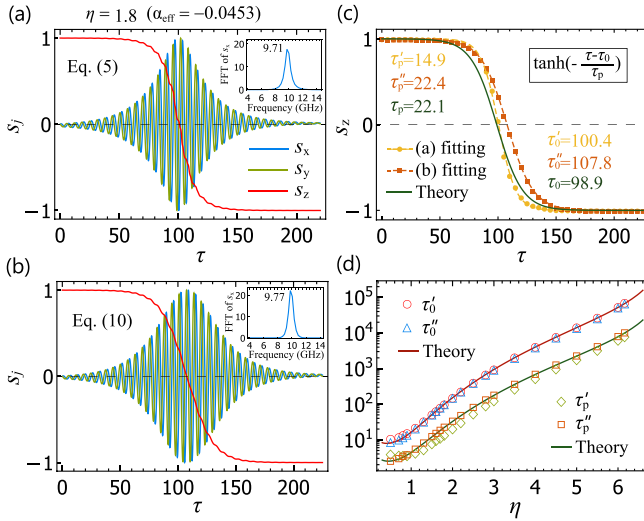


FIG. 3. Time evolution of unit spin components ( $s_x$ ,  $s_y$ ,  $s_z$ ) at detuning  $\eta = 1.8$  based on Eq. (5) (a) and Eq. (10) (b). Insets show the FFT spectrum of  $s_x$ . (c) Theoretical fittings of  $s_z$  using the hyperbolic-tangent ansatz (11) (dashed curves). The solid-green curve is the analytical formula without any fitting. (d) Numerical results of the  $\eta$  dependence of the two characteristic times  $\tau_0$  and  $\tau_p$ , comparing with formula (12) (solid curves). Time is normalized by  $\omega_m^{-1}$ .

which is reminiscent of the Walker solution for modeling the profile of  $180^\circ$  magnetic domain wall [39] by replacing the time coordinate  $\tau$  with the space coordinate  $x$ . Here  $\tau_0$  is the switching time,  $\tau_p$  represents the life-time of uniform magnons, and  $\tau = \omega_m t$ . From perturbation theory, we derive the analytical form of these two parameters

$$\tau_p = -\frac{1 + \alpha_{\text{eff}}^2}{\alpha_{\text{eff}}}, \quad \text{and} \quad \tau_0 = \tau_p \tanh^{-1} \sqrt{1 - \frac{4B_{\text{opt}}^2}{B_{\text{eff}}^2}}. \quad (12)$$

Figure 3(c) shows the time evolution of  $s_z$ . Symbols represent the numerical results, dashed curves label the theoretical fittings of ansatz (11), and the solid curve is the analytical formula without fitting. The fitted switching time  $\tau'_0 = 100.4$  ( $\tau''_0 = 107.8$ ) and magnon life-time  $\tau'_p = 14.9$  ( $\tau''_p = 22.4$ ) from Eq. (5) [Eq. (10)] compare well with the analytical formula (12) which gives  $\tau_0 = 98.9$  and  $\tau_p = 22.1$ . We further show that the analytical ansatz agrees excellently with numerical results in a broad range of detuning parameters, as plotted in Fig. 3(d).

Usually, the magnetization reversal is due to the effective field, not the damping. The underlying physics of the negative damping induced magnetization switching can be understood as follows: We use  $W$  to denote the total energy of the spin system. According to the effective LLG equation (10), we obtain its time derivative

$$\frac{dW}{dt} = -\frac{\gamma\alpha_{\text{eff}}}{1 + \alpha_{\text{eff}}^2} |\mathbf{S} \times \mathbf{B}_{\text{eff}}|^2, \quad (13)$$

where  $\mathbf{B}_{\text{eff}}$  is the time-independent effective field. For the case of a negative Gilbert damping, i.e.,  $\alpha_{\text{eff}} < 0$ , the energy change rate of the spin system is always positive. The parallel state between  $\mathbf{S}$  and  $\mathbf{B}_{\text{eff}}$  is thus unstable, and the system

seeks the energy maximum, i.e.,  $\mathbf{S}$  antiparallel with  $\mathbf{B}_{\text{eff}}$ . We therefore conclude that the flipped spin will not go back to the original direction, and it will stay in the reversed state. Numerical simulations confirm this point.

#### IV. DISCUSSION

In the above derivation, we focus on the case that the intrinsic Gilbert damping is isotropic. Our approach can also be generalized to treat the anisotropic intrinsic damping [40]. The laser beams then should match the tensor form of the damping parameter, by modulating the driving powers. The red-detuning region is appealing to cool magnons to the subtle quantum domain. Other methods, e.g., parametric driving [41], spin transfer torque [42], and antidamping spin-orbit torque [43], may generate an effective magnetic gain, but not of the Gilbert form for large-angle spin precessions. In our estimation, the optical cavity frequency is chosen around 100 THz (wavelength  $\sim 3\mu\text{m}$ , close to the laser wavelength for observing the Faraday rotation in YIG) with linewidth about 1 GHz. It requires a micrometer-size cavity with a  $Q$  factor  $\sim 10^5$ . Promising candidates include crystalline microresonators [44] and silicon nanoscale resonators [45].

Inspired by parity-time-symmetric optics [46–50], we envision a giant enhancement of the magnonic gain and an ultralow-threshold magnon lasing in a two-cavity system with balanced optical gain and loss, which is an open question for future study. While the passive parity-time symmetry has been observed by Liu *et al.* [51], the exact and imbalanced parity-time-symmetric phases are still waiting for the experimental discovery. The realization of negative Gilbert damping is helpful to resolve these issues [see Appendix C].

#### V. CONCLUSIONS

To summarize, we have proposed an optomagnonic method to generate the negative Gilbert damping in ferromagnets, by studying the parametric dynamics of a macrospin coupled with three orthogonally propagating circularly-polarized lasers in an optical cavity. We analytically derived the formula of the optical torque on the spin and identified the far-detuning condition for the torque exactly of the Gilbert form. We found a hyperbolic-tangent function reminiscent of the Walker ansatz to well describe the time-resolved spin switching when the intrinsic damping is overcome. Our findings suggest an experimentally feasible way to achieve negative Gilbert damping that is essential for substantially improving the quality factor of magnets and for exploring the non-Hermitian physics in magnonic systems.

#### ACKNOWLEDGMENTS

We acknowledge the helpful discussion with Z. Z. Sun. This work was supported by the National Natural Science Foundation of China (Grants No. 12074057, No. 11704060, and No. 11604041).

**APPENDIX A: HAMILTONIAN**

Considering a macrospin interacting with the external magnetic field, the Zeeman energy is  $H_{\text{mag}} = -\mathbf{M} \cdot \mathbf{B}$ , where the local magnetization  $\mathbf{M} = -\gamma\mathbf{S}$ , with  $\gamma = g_e\mu_B/\hbar$  the gyromagnetic ratio,  $g_e$  the electron  $g$  factor, and  $\mu_B$  being the Bohr magneton. Usually the electron  $g$  factor  $g_e \simeq 2$  and  $\gamma = 28\text{GHz/T}$ . For any right-handed coordinate system, the components of the spin operator satisfy the commutations  $[\hat{S}_x, \hat{S}_y] = i\hbar\hat{S}_z$  and its cyclic permutations. We assume that the external magnetic field is applied along  $z$  axis, i.e.,  $\mathbf{B} = -B_0\mathbf{e}_z$ , so that the Zeeman energy can be expressed as

$$H_{\text{mag}} = -\hbar\omega_m\hat{S}_z, \quad (\text{A1})$$

with  $\omega_m = \gamma B_0$  the Larmor frequency.

In the microwave regime, magnons couple resonantly with cavity photons, i.e., one magnon is converted to a photon with the same frequency and vice versa. However, the coupling between magnon and optical photon is typically a three-particle process, which accounts for the frequency mismatch and is generally parametric [28,29]. The magneto-optical interaction is essentially due to an effective permittivity tensor that depends on the magnetization of the materials. The generalized principle of symmetry of kinetic coefficients requires the off-diagonal elements satisfying  $\varepsilon_{jk}(\mathbf{M}) = \varepsilon_{kj}(-\mathbf{M})$ , and the energy lossless assumption of the sample asks for a Hermitian tensor  $\varepsilon_{jk} = \varepsilon_{kj}^*$ . Both conditions imply that the real and imaginary parts of  $\varepsilon_{jk}$  have to be symmetry and antisymmetry, respectively, as functions of  $\mathbf{M}$  [32]. We consider the linear form of the Faraday effect in an isotropic and nondispersive medium

$$\varepsilon_{jk} = \varepsilon_0\varepsilon_r\delta_{jk} + i\varepsilon_0f\epsilon_{jkl}M_l, \quad (\text{A2})$$

where  $\epsilon_{jkl}$  is the third-order Levi-Civita symbols,  $f$  is a scalar constant,  $\varepsilon_0$  and  $\varepsilon_r$  are the vacuum and relative permittivities, and subscripts  $j, k, l$  represent three directions ( $x, y, z$ ). We now focus on the optical fields with frequency close to the optical cavity mode  $\mathbf{E} = \mathbf{E}_0(t)e^{-i\omega_{\text{cav}}t}$  (the same as for magnetic component  $\mathbf{H}$ ), where  $\mathbf{E}_0(t)$  varies slowly in comparison with the factor  $e^{-i\omega_{\text{cav}}t}$ . Time-average energy density that the electromagnetic field contains in a period is

$$\bar{u} = \frac{1}{4} \sum_{jk} E_{0j}^*(t)\varepsilon_{jk}E_{0k}(t). \quad (\text{A3})$$

Substituting the tensor permittivity and integrating the volume, we obtain the expression of the total energy

$$U = \frac{1}{4}\varepsilon_0\varepsilon_r \int \mathbf{E}^* \cdot \mathbf{E} dV + \frac{i}{4}\varepsilon_0f \int \mathbf{M} \cdot (\mathbf{E}^* \times \mathbf{E}) dV, \quad (\text{A4})$$

since  $\mathbf{E}^* \cdot \mathbf{E} = \mathbf{E}_0^* \cdot \mathbf{E}_0$ . In the above equation, the first term on the right side is the steady-state photon energy, and the second one is the magneto-optical (MO) interaction. Here  $V$  is the volume of the magnet. Now, considering a plane wave propagating along  $x$  direction, one can quantize the electric fields as

$$\mathbf{E}(t) = i\sqrt{\frac{2\hbar\omega_{\text{las}}}{\varepsilon_0\varepsilon_rV}} [\hat{c}_L(t)e^{ikx}\hat{e}_L + \hat{c}_R(t)e^{ikx}\hat{e}_R], \quad (\text{A5})$$

where  $\hat{e}_{L,R} = \frac{1}{\sqrt{2}}(\hat{y} \pm i\hat{z})$  denotes the polarization direction,  $\omega_{\text{las}}$  and  $k$  are the frequency and wave vector of the laser beam, respectively. The MO Hamiltonian then becomes

$$\begin{aligned} \mathcal{H}_{\text{MO}} &= \frac{i}{4}\varepsilon_0f \int_V i\frac{2\hbar\omega_{\text{las}}}{\varepsilon_0\varepsilon_rV} (\hat{c}_R^\dagger\hat{c}_R - \hat{c}_L^\dagger\hat{c}_L)M_x dV \\ &= -\frac{f\hbar\omega_{\text{las}}}{2\varepsilon_r} (\hat{c}_R^\dagger\hat{c}_R - \hat{c}_L^\dagger\hat{c}_L)M_x. \end{aligned} \quad (\text{A6})$$

If we consider only the left-polarized driving laser, and note that  $M_x/M_s = \hat{S}_x/S$ , the MO Hamiltonian becomes

$$\mathcal{H}_{\text{MO}} = \hbar g\hat{S}_x\hat{c}^\dagger\hat{c}, \quad \text{with } g = \frac{fM_s\omega_{\text{las}}}{2S\varepsilon_r}, \quad (\text{A7})$$

where we have dropped the suffix  $L$ . The coefficient  $f$  can be obtained via the Faraday rotation per unit length  $\theta_F = \frac{fM_s\omega_{\text{las}}}{2c\sqrt{\varepsilon_r}}$  [32,36]. In the main text, we consider three identical laser beams propagating along  $x, y, z$  directions, respectively. In the rotating frame of laser frequency, corresponding to a unitary transformation  $\hat{T}(t) = \exp(-i\omega_{\text{las}}t\hat{c}^\dagger\hat{c})$ , the Hamiltonian includes the cavity photon and the off-resonant coupling becomes

$$\mathcal{H}_0 = -\hbar \sum_{j=x,y,z} (\Delta_j - g_j\hat{S}_j)\hat{c}_j^\dagger\hat{c}_j, \quad (\text{A8})$$

where  $\Delta_j = \omega_{\text{las},j} - \omega_{\text{cav}}$  is the frequency detuning between the driving laser  $\omega_{\text{las},j}$  and the cavity photon  $\omega_{\text{cav}}$ , and  $\hat{c}_j^\dagger(\hat{c}_j)$  is the creation (annihilation) operator of the optical cavity photons. By including the Zeeman energy and the external driving, we finally obtain the total Hamiltonian (2) in the main text.

**APPENDIX B: PHOTON NUMBER**

The time evolution of an operator can be obtained via the Heisenberg equation  $\dot{\hat{o}} = \frac{i}{\hbar}[\mathcal{H}, \hat{o}]$ . When performing the average of operator products, we assume  $\langle \hat{o}_1 \rangle \langle \hat{o}_2 \rangle = \langle \hat{o}_1\hat{o}_2 \rangle$ , and thus obtain Eq. (3) in the main text. To solve Eq. (3), we first solve the cavity photons by expanding the cavity photon operator as  $c_j(t) \approx c_{j0}(t) + c_{j1}(t) + \dots$ , in orders of  $\hat{S}_j$ . This approach can be well justified that the cavity photon dynamics is much faster than spin dynamics [29]. Similar treatments have been adopted in optomechanical systems to derive the mechanical gain [52–54]. To the first order of  $c_{j0}(t) \sim S_j$ , Eq. (3a) gives

$$0 = (i\Delta_j - \kappa_j)c_{j0}(t) - ig_jS_jc_{j0}(t) + A_j. \quad (\text{B1})$$

To the second order of  $c_{j1}(t) \sim \hat{S}_j$ , we have

$$\dot{c}_{j0} = (i\Delta_j - \kappa_j)c_{j1} - ig_jS_jc_{j1}. \quad (\text{B2})$$

One therefore obtains Eq. (4) in the main text. It is noted that the three spin components are not independent when we discuss the spin dynamics. However, the photon dynamics is purely linear, as seen in Eq. (3a) in the main text. According to the Faraday interaction form, photons propagating along different directions couple with different spin components. For example, photons propagating along  $x$  direction, i.e.,  $c_x$ , depends only on component  $S_x$ . Similarly,  $c_y$  only couples with  $S_y$  and  $c_z$  only couples with  $S_z$ . Our derivations from Eq. (A4) to Eq. (A7) have demonstrated this point (taking the

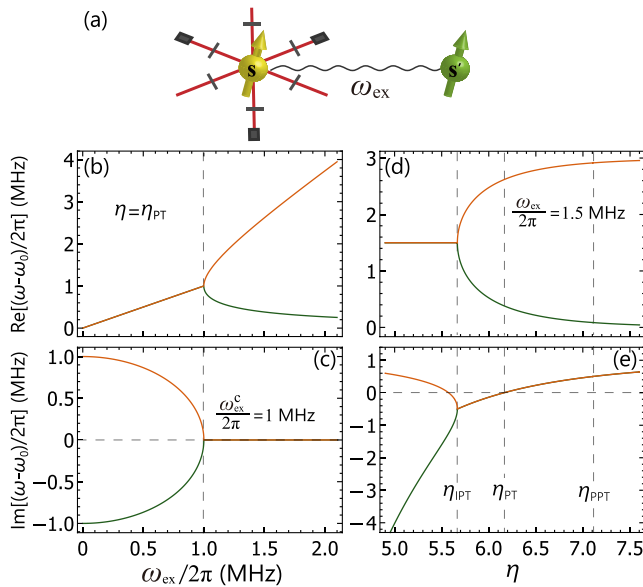


FIG. 4. (a) Spin dimer consisting of an optically pumped spin  $\mathbf{s}$  and a purely lossy one  $\mathbf{s}'$ . Evolution of eigenfrequencies vs the exchange coupling (b,c) at the detuning  $\eta_{PT} = 6.16$ , and vs the detuning parameter (d,e) at the exchange coupling  $\omega_{ex}/2\pi = 1.5$  MHz.

$x$  component as an example). This also explains why we adopt three orthogonal laser beams to drive the spin in our proposal. By keeping up to the first-order terms, we can finally derive the formula of photon number in the cavity

$$\begin{aligned}
 n_j(t) &= |c_j(t)|^2 \approx |c_{j0}|^2 + 2\text{Re}[c_{j0}^* c_{j1}] \\
 &= \frac{A_j^2}{(\Delta_j - g_j S_j)^2 + \kappa_j^2} - \frac{4\kappa_j A_j^2 g_j (\Delta_j - g_j S_j)}{[(\Delta_j - g_j S_j)^2 + \kappa_j^2]^3} \dot{S}_j.
 \end{aligned}
 \tag{B3}$$

### APPENDIX C: $\mathcal{PT}$ SYMMETRY IN SPIN DIMERS

We have shown that under proper conditions, one can realize the Gilbert-type magnetic gain, which is essential for observing  $\mathcal{PT}$  symmetry in purely magnetic structures. Next, we consider the optically pumped spin  $\mathbf{S}$  interacting with a lossy one  $\mathbf{S}'$ , as shown in Fig. 4(a). The coupled spin dynamics is described by the LLG equation

$$\dot{\mathbf{s}} = -\gamma \mathbf{s} \times \mathbf{B}_{\text{eff}} + \omega_{ex} \mathbf{s} \times \mathbf{s}' + \alpha_{\text{eff}} \dot{\mathbf{s}} \times \mathbf{s}, \tag{C1a}$$

$$\dot{\mathbf{s}}' = -\gamma \mathbf{s}' \times \mathbf{B}'_{\text{eff}} + \omega_{ex} \mathbf{s}' \times \mathbf{s} + \alpha' \dot{\mathbf{s}}' \times \mathbf{s}', \tag{C1b}$$

where  $\mathbf{s}^{(\prime)} \equiv \mathbf{S}^{(\prime)}/S$  is the unit spin vector. Since the optically induced magnetic field is the same order of magnitude with the geomagnetic field (much smaller than  $B_0$ ), it can be safely ignored. Spin  $\mathbf{s}'$  is exchange coupled to the optically pumped spin  $\mathbf{s}$ , and suffers an intrinsic Gilbert damping. If  $\alpha_{\text{eff}} = -\alpha$ , the two-spin system satisfies the  $\mathcal{PT}$  symmetry: Eqs. (C1) are invariant in the combined operation of the parity  $\mathcal{P}$  ( $\mathbf{s} \leftrightarrow \mathbf{s}'$  and  $\mathbf{B}_{\text{eff}} \leftrightarrow \mathbf{B}'_{\text{eff}}$ ) and the time reversal  $\mathcal{T}$  ( $t \rightarrow -t$ ,  $\mathbf{s} \rightarrow -\mathbf{s}$ ,  $\mathbf{s}' \rightarrow -\mathbf{s}'$ ,  $\mathbf{B}_{\text{eff}} \rightarrow -\mathbf{B}_{\text{eff}}$ , and  $\mathbf{B}'_{\text{eff}} \rightarrow -\mathbf{B}'_{\text{eff}}$ ).

Assuming a harmonic time-dependence for the small-angle spin precession  $s_{x,y}(t) = s_{x,y} e^{i\omega t}$  with  $|s_{x,y}| \ll 1$ , one can solve the eigenspectrum of Eqs. (C1). By tuning the spin-spin coupling strength  $\omega_{ex}$ , we observe a transition from exact  $\mathcal{PT}$  phase to the broken  $\mathcal{PT}$  phase, separated by the EP at  $\omega_{ex}^c/2\pi = 1$  MHz for  $\eta = \eta_{PT} = 6.16$ , as shown in Figs. 4(b) and 4(c). Interestingly, the unequal gain and loss, i.e.,  $\alpha_{\text{eff}} < 0$  and  $\alpha_{\text{eff}} \neq -\alpha$ , leads to an imbalanced parity-time ( $\mathcal{IPT}$ )-symmetry. In this region ( $\eta > \eta_{PT} = 5.66$ ), the eigenfrequencies have different real parts but share the identical imaginary one, as plotted in Fig. 4(d). Although the gain and loss are not equal for  $\mathcal{IPT}$ , one can still observe the exceptional point where the magnetic sensitivity can be significantly enhanced [21]. A passive parity-time ( $\mathcal{PPT}$ )-symmetry is further identified when  $\alpha_{\text{eff}} > 0$ . In such case ( $\eta > \eta_{PPT} = 7.11$ ), the imaginary part of both branches is smaller than their intrinsic damping [see Fig. 4(e)].

- [1] T. L. Gilbert, A phenomenological theory of damping in ferromagnetic materials, *IEEE Trans. Magn.* **40**, 3443 (2004).
- [2] Y. Cao and P. Yan, Role of atomic spin-mechanical coupling in the problem of a magnetic biocompass, *Phys. Rev. E* **97**, 042409 (2018).
- [3] S. Parkin, M. Hayashi, and L. Thomas, Magnetic domain-wall racetrack memory, *Science* **320**, 190 (2008).
- [4] Z.-X. Li, Y. Cao, and P. Yan, Topological insulators and semimetals in classical magnetic systems, *Phys. Rep.* **915**, 1 (2021).
- [5] B. Hillebrands and A. Thiaville (eds.), *Spin Dynamics in Confined Magnetic Structures I* (Springer-Verlag, Berlin, 2006).
- [6] Y. Kajiwara, K. Harii, S. Takahashi, J. Ohe, K. Uchida, M. Mizuguchi, H. Umezawa, H. Kawai, K. Ando, K. Takanashi, S. Maekawa, and E. Saitoh, Transmission of electrical signals by spin-wave interconversion in a magnetic insulator, *Nature (London)* **464**, 262 (2010).
- [7] V. Cherepanov, I. Kolokolov, and V. L'vov, The saga of YIG: Spectra, thermodynamics, interaction and relaxation of magnons in a complex magnet, *Phys. Rep.* **229**, 81 (1993).
- [8] T. J. Kippenberg, R. Holzwarth, and S. A. Diddams, Microresonator-based optical frequency combs, *Science* **332**, 555 (2011).
- [9] M. Reagor, W. Pfaff, C. Axline, R. W. Heeres, N. Ofek, K. Sliwa, E. Holland, C. Wang, J. Blumoff, K. Chou, M. J. Hatridge, L. Frunzio, M. H. Devoret, L. Jiang, and R. J. Schoelkopf, Quantum memory with millisecond coherence in circuit QED, *Phys. Rev. B* **94**, 014506 (2016).
- [10] Z. Wang, H. Y. Yuan, Y. Cao, Z.-X. Li, R. A. Duine, and P. Yan, Magnonic Frequency Comb through Nonlinear Magnon-Skyrmion Scattering, *Phys. Rev. Lett.* **127**, 037202 (2021).
- [11] M. C. Hickey and J. S. Moodera, Origin of Intrinsic Gilbert Damping, *Phys. Rev. Lett.* **102**, 137601 (2009).

- [12] H. B. Callen, in *Fluctuation, Relaxation, and Resonance in Magnetic Systems*, edited by D. ter Haar (Oliver & Boyd, London, 1962), p. 176.
- [13] C. Vittoria, S. D. Yoon, and A. Widom, Relaxation mechanism for ordered magnetic materials, *Phys. Rev. B* **81**, 014412 (2010).
- [14] A. B. Oliveira, R. L. Rodríguez-Suárez, M. A. Correa, F. Bohn, S. A. Raza, R. L. Sommer, and C. Chesman, Filtering magnetic relaxation mechanisms of YIG(001) thin films using ferromagnetic resonance, *J. Magn. Magn. Mater.* **507**, 166851 (2020).
- [15] H. Huebl, C. W. Zollitsch, J. Lotze, F. Hocke, M. Greifenstein, A. Marx, R. Gross, and S. T. B. Goennenwein, High Cooperativity in Coupled Microwave Resonator Ferrimagnetic Insulator Hybrids, *Phys. Rev. Lett.* **111**, 127003 (2013).
- [16] Y. Tabuchi, S. Ishino, T. Ishikawa, R. Yamazaki, K. Usami, and Y. Nakamura, Hybridizing Ferromagnetic Magnons and Microwave Photons in the Quantum Limit, *Phys. Rev. Lett.* **113**, 083603 (2014).
- [17] X. Zhang, C.-L. Zou, L. Jiang, and H. X. Tang, Strongly Coupled Magnons and Cavity Microwave Photons, *Phys. Rev. Lett.* **113**, 156401 (2014).
- [18] L. Bai, M. Harder, Y. P. Chen, X. Fan, J. Q. Xiao, and C.-M. Hu, Spin Pumping in Electro-dynamically Coupled Magnon-Photon Systems, *Phys. Rev. Lett.* **114**, 227201 (2015).
- [19] Y. Cao, P. Yan, H. Huebl, S. T. B. Goennenwein, and G. E. W. Bauer, Exchange magnon-polaritons in microwave cavities, *Phys. Rev. B* **91**, 094423 (2015).
- [20] Y. Tabuchi, S. Ishino, A. Noguchi, T. Ishikawa, R. Yamazaki, K. Usami, and Y. Nakamura, Coherent coupling between a ferromagnetic magnon and a superconducting qubit, *Science* **349**, 405 (2015).
- [21] Y. Cao and P. Yan, Exceptional magnetic sensitivity of PT-symmetric cavity magnon polaritons, *Phys. Rev. B* **99**, 214415 (2019).
- [22] B. Z. Rameshti, S. V. Kusminskiy, J. A. Haigh, K. Usami, D. Lachance-Quirion, Y. Nakamura, C.-M. Hu, H. X. Tang, G. E. W. Bauer, and Y. M. Blanter, Cavity magnonics, [arXiv:2106.09312](https://arxiv.org/abs/2106.09312).
- [23] H. Y. Yuan, Y. Cao, A. Kamra, R. A. Duine, and P. Yan, Quantum magnonics: When magnon spintronics meets quantum information science, [arXiv:2111.14241](https://arxiv.org/abs/2111.14241).
- [24] A. Osada, A. Gloppe, R. Hisatomi, A. Noguchi, R. Yamazaki, M. Nomura, Y. Nakamura, and K. Usami, Brillouin Light Scattering by Magnetic Quasivortices in Cavity Optomagnonics, *Phys. Rev. Lett.* **120**, 133602 (2018).
- [25] R. W. Andrews, R. W. Peterson, T. P. Purdy, K. Cicak, R. W. Simmonds, C. A. Regal, and K. W. Lehnert, Bidirectional and efficient conversion between microwave and optical light, *Nat. Phys.* **10**, 321 (2014).
- [26] X. Zhang, N. Zhu, C.-L. Zou, and H. X. Tang, Optomagnonic Whispering Gallery Microresonators, *Phys. Rev. Lett.* **117**, 123605 (2016).
- [27] S. Sharma, Y. M. Blanter, and G. E. W. Bauer, Optical Cooling of Magnons, *Phys. Rev. Lett.* **121**, 087205 (2018).
- [28] T. Liu, X. Zhang, H. X. Tang, and M. E. Flatté, Optomagnonics in magnetic solids, *Phys. Rev. B* **94**, 060405(R) (2016).
- [29] S. V. Kusminskiy, H. X. Tang, and F. Marquardt, Coupled spin-light dynamics in cavity optomagnonics, *Phys. Rev. A* **94**, 033821 (2016).
- [30] H. Yang, C. Wang, T. Yu, Y. Cao, and P. Yan, Antiferromagnetism Emerging in a Ferromagnet with Gain, *Phys. Rev. Lett.* **121**, 197201 (2018).
- [31] T. Yu, H. Yang, L. Song, P. Yan, and Y. Cao, Higher-order exceptional points in ferromagnetic trilayers, *Phys. Rev. B* **101**, 144414 (2020).
- [32] L. D. Landau and E. M. Lifshitz, *Electrodynamics of Continuous Media*, 2nd ed. (Pergamon, Oxford, UK, 1984).
- [33] There are various origins for the intrinsic Gilbert damping. For ferromagnetic insulators, the leading one comes from the magnetoelastic (or spin-phonon) coupling. From a more general perspective, one can exactly derive the intrinsic Gilbert damping by considering a microscopic coupling between the spin and a bosonic thermal bath with the Markovian approximation. Such a treatment can be found, for instance, in Ref. [34].
- [34] A. Rückriegel and P. Kopietz, Rayleigh-Jeans Condensation of Pumped Magnons in Thin-Film Ferromagnets, *Phys. Rev. Lett.* **115**, 157203 (2015).
- [35] K. Sadhana, R. S. Shinde, and S. R. Murthy, Synthesis of nanocrystalline YIG using microwave-hydrothermal method, *Int. J. Mod. Phys. B* **23**, 3637 (2009).
- [36] R. W. Cooper, W. A. Crossley, J. L. Page, and R. F. Pearson, Faraday rotation in YIG and TbIG, *J. Appl. Phys.* **39**, 565 (1968).
- [37] R. Kikuchi, On the minimum of magnetization reversal time, *J. Appl. Phys.* **27**, 1352 (1956).
- [38] Z. Z. Sun and X. R. Wang, Fast magnetization switching of Stoner particles: A nonlinear dynamics picture, *Phys. Rev. B* **71**, 174430 (2005).
- [39] N. L. Schryer and L. R. Walker, The motion of 180° domain walls in uniform dc magnetic fields, *J. Appl. Phys.* **45**, 5406 (1974).
- [40] L. Chen, S. Mankovsky, S. Wimmer, M. A. W. Schoen, H. S. Körner, M. Kronseder, D. Schuh, D. Bougeard, H. Ebert, D. Weiss, and C. H. Back, Emergence of anisotropic Gilbert damping in ultrathin Fe layers on GaAs(001), *Nat. Phys.* **14**, 490 (2018).
- [41] J. M. Lee, T. Kottos, and B. Shapiro, Macroscopic magnetic structures with balanced gain and loss, *Phys. Rev. B* **91**, 094416 (2015).
- [42] K. Xia, P. J. Kelly, G. E. W. Bauer, A. Brataas, and I. Turek, Spin torques in ferromagnetic/normal-metal structures, *Phys. Rev. B* **65**, 220401(R) (2002).
- [43] B. Divinskiy, S. Urazhdin, S. O. Demokritov, and V. E. Demidov, Controlled nonlinear magnetic damping in spin-Hall nano-devices, *Nat. Commun.* **10**, 5211 (2019).
- [44] C. Y. Wang, T. Herr, P. Del'Haye, A. Schliesser, J. Hofer, R. Holzwarth, T. W. Hänsch, N. Picqué, and T. J. Kippenberg, Mid-infrared optical frequency combs at 2.5 mm based on crystalline microresonators, *Nat. Commun.* **4**, 1345 (2013).
- [45] J. Chan, T. P. M. Alegre, A. H. Safavi-Naeini, J. T. Hill, A. Krause, S. Gröblacher, M. Aspelmeyer, and O. Painter, Laser cooling of a nanomechanical oscillator into its quantum ground state, *Nature (London)* **478**, 89 (2011).
- [46] L. Feng, Y.-L. Xu, W. S. Fegadolli, M.-H. Lu, J. E. B. Oliveira, V. R. Almeida, Y.-F. Chen, and A. Scherer, Experimental demonstration of a unidirectional reflectionless parity-time

- metamaterial at optical frequencies, *Nat. Mater.* **12**, 108 (2012).
- [47] B. Peng, S. K. Özdemir, F. Lei, F. Monifi, M. Gianfreda, G. L. Long, S. Fan, F. Nori, C. M. Bender, and L. Yang, Parity–time-symmetric whispering-gallery microcavities, *Nat. Phys.* **10**, 394 (2004).
- [48] A. Guo, G. J. Salamo, D. Duchesne, R. Morandotti, M. Volatier-Ravat, V. Aimez, G. A. Sivilogou, and D. N. Christodoulides, Observation of PT-Symmetry Breaking in Complex Optical Potentials, *Phys. Rev. Lett.* **103**, 093902 (2009).
- [49] W. Chen, S. K. Özdemir, G. Zhao, J. Wiersig, and L. Yang, Exceptional points enhance sensing in an optical microcavity, *Nature (London)* **548**, 192 (2017).
- [50] H. Hodaie, A. U. Hassan, S. Wittek, H. Garcia-Gracia, R. El-Ganainy, D. N. Christodoulides, and M. Khajavikhan, Enhanced sensitivity at higher-order exceptional points, *Nature (London)* **548**, 187 (2017).
- [51] H. Liu, D. Sun, C. Zhang, M. Groesbeck, R. Mclaughlin, and Z. V. Vardeny, Observation of exceptional points in magnonic parity-time symmetry devices, *Sci. Adv.* **5**, eaax9144 (2019).
- [52] S. Mancini and P. Tombesi, Quantum noise reduction by radiation pressure, *Phys. Rev. A* **49**, 4055 (1994).
- [53] I. S. Grudinin, H. Lee, O. Painter, and K. J. Vahala, Phonon Laser Action in a Tunable Two-Level System, *Phys. Rev. Lett.* **104**, 083901 (2010).
- [54] M. Aspelmeyer, T. J. Kippenberg, and F. Marquardt, Cavity optomechanics, *Rev. Mod. Phys.* **86**, 1391 (2014).